

Minerva Access is the Institutional Repository of The University of Melbourne

Author/s:

Lee, FT;Burvenich, IJG;Guo, N;Kocovski, P;Tochon-Danguy, H;Ackermann, U;O'Keefe, GJ;Gong, S;Rigopoulos, A;Liu, Z;Gan, HK;Scott, AM

Title:

l-Tyrosine Confers Residualizing Properties to a d-Amino Acid-Rich Residualizing Peptide for Radioiodination of Internalizing Antibodies

Date:

2016-06-02

Citation:

Lee, F. T., Burvenich, I. J. G., Guo, N., Kocovski, P., Tochon-Danguy, H., Ackermann, U., O'Keefe, G. J., Gong, S., Rigopoulos, A., Liu, Z., Gan, H. K. & Scott, A. M. (2016). l-Tyrosine Confers Residualizing Properties to a d-Amino Acid-Rich Residualizing Peptide for Radioiodination of Internalizing Antibodies. *Molecular Imaging*, 15, pp.1-9. <https://doi.org/10.1177/1536012116647535>.

Persistent Link:

<https://hdl.handle.net/11343/260406>

License:

CC BY-NC

L-Tyrosine Confers Residualizing Properties to a D-Amino Acid-Rich Residualizing Peptide for Radioiodination of Internalizing Antibodies

Fook T. Lee, PhD¹, Ingrid J. G. Burvenich, PhD¹, Nancy Guo, MBBS, MSc¹, Pece Kocovski, BSc (Honors)¹, Henri Tochon-Danguy, PhD², Uwe Ackermann, PhD², Graeme J. O'Keefe, PhD², Sylvia Gong, PhD², Angela Rigopoulos, BSc, MSc¹, Zhanqi Liu, MBBS, PhD¹, Hui K. Gan, MBBS, FRACP, PhD¹, and Andrew M. Scott, MBBS, FRACP, MD^{1,2}

Abstract

Purpose: The aims of the study were to develop and evaluate a novel residualizing peptide for labeling internalizing antibodies with ¹²⁴I to support clinical development using immuno-positron emission tomography (PET).

Methods: The anti-epidermal growth factor receptor antibody ch806 was radiolabeled directly or indirectly with isotopes and various residualizing peptides. Azido-derivatized radiolabeled peptides were conjugated to dibenzylcyclooctyne-derivatized ch806 antibody via click chemistry. The radiochemical purities, antigen-expressing U87MG.de2-7 human glioblastoma cell-binding properties, and targeting of xenografts at 72 hours post injection of all radioconjugates were compared. Biodistribution of ¹²⁴I-PEG₄-tptddYddtpt-ch806 and immuno-PET imaging were evaluated in tumor-bearing mice.

Results: Biodistribution studies using xenografts at 72 hours post injection showed that ¹³¹I-PEG₄-tptddYddtpt-ch806 tumor uptake was similar to ¹¹¹In-CHX-A''-DTPA-ch806. ¹²⁵I-PEG₄-tptddyddtpt-ch806 showed a lower tumor uptake value but higher than directly labeled ¹²⁵I-ch806. ¹²⁴I-PEG₄-tptddYddtpt-ch806 was produced at 23% labeling efficiency, 98% radiochemical purity, 25.9 MBq/mg specific activity, and 64% cell binding in the presence of antigen excess. Tumor uptake for ¹²⁴I-PEG₄-tptddYddtpt-ch806 was similar to ¹¹¹In-CHX-A''-DTPA-ch806. High-resolution immuno-PET/magnetic resonance imaging of tumors showed good correlation with biodistribution data.

Conclusions: The mixed D/L-enantiomeric peptide, DThr-DPro-DThr-DAsp-DAsp-Tyr-DAsp-DAsp-DThr-DPro-DThr, is suitable for radiolabeling antibodies with radiohalogens such as ¹²⁴I for high-resolution immuno-PET imaging of tumors and for evaluation in early-phase clinical trials.

Keywords

residualizing peptide, iodine-124, antibodies, internalization, immuno-PET

Introduction

Monoclonal antibodies and antibody drug conjugates are now playing an important role in the management of patients with cancer.^{1,2} In order to aid clinical antibody development, the development of immuno-SPECT and immuno-positron emission tomography (PET) reagents can provide a noninvasive technique to aid in patient selection for antibody therapy either by confirming the presence of antibody binding to multiple tumor lesions or by

¹ Tumour Targeting Program, Ludwig Institute For Cancer Research and Olivia Newton-John Cancer Research Institute, Heidelberg, Victoria, Australia

² Department of Nuclear Medicine and Centre for PET, Austin Health, Heidelberg, Victoria, Australia

Submitted: 24/03/2015. Revised: 28/08/2015. Accepted: 17/03/2016.

Corresponding Author:

Fook T. Lee, Tumour Targeting Program, Olivia Newton-John Cancer Research Institute, Austin Health, Studley Road, Heidelberg, Victoria 3084, Australia.

Email: ft.lee@onjcri.org.au



determining the delivered radiation dose in patients planned for radioimmunotherapy.³⁻⁵

The epidermal growth factor receptor (EGFR) belongs to the ErbB/HER tyrosine kinase receptor family, which consists of 4 receptors (HER1-4). Overexpression of EGFR during tumorigenesis has been associated with many epithelial cancers, correlating with poor disease progression and poor clinical outcome, and makes this receptor an attractive target for therapeutic antibodies.^{6,7} One of the EGFR-targeting antibodies that is currently undergoing clinical development, 806, is able to distinguish tumor cells with an amplified/overexpressed EGFR phenotype from normal cells having wild-type levels of EGFR expression and also targets a truncated form of EGFR (EGFRvIII).^{8,9} The EGFR is internalized following ligand binding or antibody binding.⁹

Immuno-SPECT reagents, ¹²⁵I- and ¹¹¹In-CHX-A''-DTPA-labeled chimeric 806 (ch806)¹⁰, and more recently, ¹²⁴I-IMP-R4-ch806 for immuno-PET,¹¹ have been developed and characterized. Both ¹¹¹In-CHX-A''-DTPA- and ¹²⁴I-IMP-R4-ch806 showed good tumor uptake and tumor retention in tumor-bearing mice, while ¹²⁵I-ch806 showed reduced tumor uptake and retention, most likely due to the rapid diffusion of radioiodinated catabolites out of the lysosomes. Excellent tumor uptake of ¹¹¹In-CHX-A''-DTPA-ch806 was also evident in patients entered into a Phase I clinical trial, and more recently ABT-806i (¹¹¹In-labeled humanized ABT-806, formerly mAb806) has been successfully explored in a Phase I trial.^{12,13} Because of its higher spatial resolution, better signal-to-noise ratio, and straightforward data quantification, the development of a clinically suitable immuno-PET radiopharmaceutical to aid clinical development of 806 is preferable.⁵

A large proportion of anticancer monoclonal antibodies are internalized after binding to cell surface antigens and translocated to lysosomes where proteolytic digestion occurs.^{14,15} When such antibodies are labeled directly with radiohalogens such as ¹²⁴I via endogenous tyrosine residues, resultant radiocatabolites diffuse out of the lysosomes, resulting in reduced overall uptake and retention in tumors. Various residualizing ligands for radioiodination, including nonmetabolizable carbohydrate-tyramine adducts,¹⁶⁻²¹ aromatic acylation agents bearing substituents that will remain charged at lysosomal pH,²²⁻²⁴ short D-amino acid peptides,^{25,26} and DTPA-appended D-amino acid containing peptides,^{27,28} have been developed with varying degrees of success and ease of use. These residualizing ligands resist lysosomal degradation and are trapped within the cell after antibody proteolysis. This approach utilizing ¹²⁴I for immuno-PET has the potential advantage of less bone uptake compared to ⁸⁹Zr-chelate-antibody approaches. Normal organ uptake of ⁸⁹Zr-antibodies are in general dependent on the antibody native amino acid sequences, and how the antibody is purified may be also important.

The goal of this study was to design and evaluate novel peptides for residualizing radioiodine labeling based on the observation that flanking a pentapeptide with 3 D-amino acid sequences of DThr-DPro-DThr on both the N- and the C-terminals of the peptide protects the core pentapeptide from proteolytic breakdown in serum and lysosomal preparations in

vitro.²⁹ Peptides were derivatized in the N-terminus with azido-PEG₄-NHS, radioiodinated, and "clicked" onto dibenzylcyclooctyne (DBCO)-derivatized ch806 via click chemistry (see Figure 1). Paired-label comparisons of tumor uptake in BALB/c *nu/nu* mice bearing EGFR-overexpressing U87MG.de2-7 human glioblastoma xenografts were made at 72 hours post injection to compare ¹³¹I-PEG₄-DThr-DPro-DThr-DAsp-DAsp-Tyr-DAsp-DAsp-DThr-DPro-DThr (¹³¹I-PEG₄-tptddYddtpt) directly to radioiodinated ¹²⁵I-ch806, and the all-D peptide ¹²⁵I-PEG₄-DThr-DPro-DThr-DAsp-DAsp-DTyr-DAsp-DAsp-DThr-DPro-DThr (¹²⁵I-PEG₄-tptddyddtpt) to ¹¹¹In-labeled ch806. This is an advantage, as the 2-paired isotopes can be detected simultaneously using appropriate windows on the gamma counter. The D/L-enantiomeric peptide PEG₄-tptddYddtpt showed the highest residualizing properties and was selected for radioiodination of ch806 using ¹²⁴I. ¹²⁴I-PEG₄-tptddYddtpt-ch806 was further evaluated for targeting EGFR-overexpressing U87MG.de2-7 human glioblastoma cells in vitro and in vivo.

Materials and Methods

All analytical grade reagents, except when stated, were obtained from Merck Pty Ltd (Melbourne, Australia). ¹²⁵I and ¹³¹I in 0.02 N NaOH were purchased from PerkinElmer (Sydney, Australia). ¹¹¹In in 0.01 N HCl was purchased from Mallinckrodt (Sydney, Australia). ¹²⁴I in 0.02 N NaOH (>10 mCi/mL) was prepared in house by the Austin Cyclotron (Heidelberg, Australia). Radioactivity was measured either with a dose calibrator (Biodex Atomlab-100; Brookhaven, New York) or Wizard gamma counter (PerkinElmer) with appropriate settings.

Peptide Synthesis

Various peptides, tptddyddtpt (all D-enantiomeric, 11-mer peptide containing threonine, proline, aspartic acid, tyrosine residues) and tptddYddtpt (as previous, except substitution with L-Tyrosine) were synthesized, derivatized using azido-PEG₄-NHS, and purified by Mimotopes (Melbourne, Australia).

Antibodies and Cells

The antibody ch806 targets EGFR that is overexpressed, amplified, or mutated (de2-7 EGFR or EGFRvIII) and was produced in house as described previously.¹¹ The U87MG.de2-7 glioblastoma cells that overexpress mutated EGFR were obtained and cultured as described previously.¹⁰

Antibody Conjugation and Radiolabeling

Ch806 was iodinated directly using ¹²⁵I and indirectly with ¹¹¹In via the bifunctional metal ion chelate CHX-A''-DTPA (Macrocyclics Inc, Dallas, Texas) as described previously.³⁰ For radioiodination using ¹²⁵I, reaction was performed using pH-neutralized isotopes, catalyzed by IODO-GEN precoated glass beads (Thermo Fisher Scientific Pierce, Rockford, Illinois).¹¹ After a brief 10-minute incubation period, the reaction was purified through a desalting column (Sephadex G50-80;

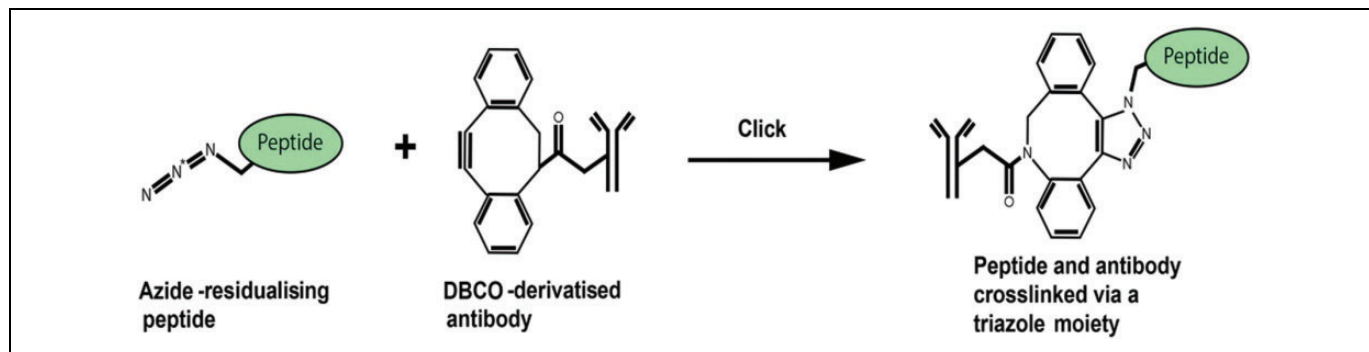


Figure 1. Schematic diagram indicating conjugation of radiolabeled azide-derivatized residualizing peptide to a DBCO-derivatised antibody via click chemistry. DBCO indicates dibenzylcyclooctyne.

Sigma-Aldrich, Sydney, Australia) equilibrated with phosphate-buffered saline.

For indirect iodination, the ch806 was derivatized with DBCO-PEG₄-NHS ester (DBCO-PEG₄-NHS, Jena Biosciences, Jena, Germany) at a 5:1 mole ratio according to the manufacturer's instructions. Azido-derivatized peptides were radiolabeled with one of ¹²⁵I, ¹³¹I, or ¹²⁴I before attachment to DBCO-PEG₄-ch806 (see Supplemental Materials and Methods).

Radiochemical Purity

Radiochemical purity of purified radiolabeled ch806 was analyzed by instant thin-layer chromatography silica gel-impregnated glass fibers (ITLC-SG) using 10% trichloroacetic acid as mobile phase. Radiochemical purity was confirmed by size exclusion chromatography (SEC). A SEC analysis was performed on a Superdex 200 HR10/30 column (Ge Healthcare Australia, Parramatta, Australia) at a flow rate of 0.14 mL/min and fraction size of 3.6 mL. The elution buffer was phosphate-buffered saline at pH 7.4.

Immunoreactivity Assays

The immunoreactivity of radiolabeled ch806 was initially determined using the Lindmo and Scatchard assay as described previously.¹¹ In these assays, 20 ng of radiolabeled ch806 were mixed with an increasing cell concentration from 0 to 1×10^7 U87MG.de2-7 cells in 1.0 mL of media.

After constant mixing for 45 minutes, the cells were washed by repeated centrifugation and cell pellets counted together with suitable standards. For Scatchard assays, 20 ng of radioconjugates were mixed with an increasing protein concentration from 20 ng to 10 μ g in 1.0 mL of media containing 1×10^6 cells. Subsequently, a single point binding assay using a fixed amount of 20 ng of radioconjugates and containing 10×10^6 U87MG.de2-7 cells in 1.0 mL of media, representing conditions for antigen excess, was employed to compare the immunoreactivities of various radiolabeled ch806. The stability of radioconjugate was determined by incubating 15 μ g of radioconjugate in a total volume of 75 μ L human serum and incubating at 37°C over a period of 7 days. An aliquot of the mixture was diluted

for radiochemical purity analysis and single-point immunoreactivity assays (10×10^6 cells) on days 0, 3, and 7.

Animals and Xenografts

The U87MG.de2-7 cells were cultured as described previously.¹¹ Cells were harvested at the point of confluence using phosphate-buffered saline/0.05% EDTA (w/v) and resuspended in media. For tumor injections, 3.0×10^6 U87MG.de2-7 cells in 0.1 mL of phosphate-buffered saline were injected subcutaneously into the flanks of 4- to 5-week-old female BALB/c nude mice. Tumor sizes were measured using the formula $(L \times W^2) \times 0.5$, where length (L) was the maximum measurement of the tumor and width (W) was the measurement perpendicular to it. Tumors started to develop 1 week after injection, and mice were used when tumors were greater than 160 mm³. All animal studies were approved by the Austin Health Animal Ethics Committee (Austin Health, Heidelberg, Australia).

Biodistribution Studies

To compare in vivo properties of various ch806 radioconjugates, sterile filtered mixtures of 5.0 μ g ¹²⁵I-ch806 (6 μ Ci or 222 kBq) and 5.0 μ g ¹³¹I-PEG₄-tptddYddtpt-ch806 (3 μ Ci or 111 kBq) or 5.0 μ g ¹²⁵I-PEG₄-tptddyddtpt (6.5 μ Ci or 240.5 kBq) and 5.0 μ g ¹¹¹In-CHX-A''-DTPA-ch806 (6 μ Ci or 222 kBq), in 0.1 mL phosphate-buffered saline/0.05% human serum albumin, were injected in BALB/c nude mice bearing U87MG.de2-7 xenografts (n = 5). Mice were killed at 72 hours after injection by isoflurane (Forane, Baxter Australia, Old Toongabbie, Australia) overinhalation, followed by exsanguination via cardiac puncture to collect blood. Tumors and organs (skin, liver, spleen, intestine, stomach, kidneys, brain, bone [femur], lungs, and heart) were harvested immediately, blot dried, and weighed (Sartorius Basic Balance, Germany). All samples were counted for radioactivity in a gamma scintillation counter (Wizard, PerkinElmer, Sydney, Australia) set with appropriate dual channel windows. Standards of a known radioactive concentration prepared from the injected materials were counted each time with blood and tissue samples enabling

calculations to be corrected for the physical decay of the isotopes. Results of labeled antibody distribution over time were expressed as percentage of injected dose per gram (% ID/g) [(counts per minute for tissue sample/counts per minute for standard] \times 100 /weight in grams).

In addition, a full biodistribution study was conducted by injecting 5.0 μ g of ^{124}I -PEG₄-tptddYddtpt-ch806 (3.5 μ Ci or 129.5 kBq) in U87MG.de2-7 tumor-bearing mice. At 2, 24, 48, 72, 120 and 168 hours after injection, 5 mice were killed and blood and tissues were collected. Blood clearance kinetics were determined using a pharmacokinetic curve-fitting program (WinNonlin phoenix, Pharsight Corp, California).

Positron Emission Tomography/Magnetic Resonance Imaging

A separate group of 5 U87MG.de2-7 tumor-bearing mice were injected intravenously via the tail vein with 74 μ g of ^{124}I -PEG₄-tptddYddtpt-ch806 (1.92 MBq). PET/magnetic resonance imaging (PET/MRI) was performed on a nanoScan PET/magnetic resonance (MR; Mediso, Budapest, Hungary) on 2 mice at the ACRF Centre for Translational Cancer Therapeutics and Imaging (Melbourne, Australia) at 2, 72, and 168 hours after injection. Mice were anaesthetized with isoflurane via inhalation and maintained in a MINERVE anesthetic assembly (Equipelement Vétérinaire MINERVE, Esternay, France). The mouse was then transferred to 1 single-mouse anesthesia/imaging closet chamber for MRI scans in tail-first supine position, followed by a 30-minute PET static scan at 2, 72, and 168 hours after injection. All PET raw data were decay, dead time, random, and attenuation corrected and were reconstructed into volumetric images with a transaxial matrix size of 255 \times 255 using the built-in quasi-Monte Carlo simulation algorithm combined with stochastic iteration and filtered sampling. The voxel dimension in the reconstructed images was 0.4 \times 0.4 \times 0.4 mm. The mice were culled and blood and tissues obtained for radioactive counting together with standards.

Statistical Analysis

Data are presented as mean \pm standard deviation. Statistical analysis was performed using a paired *t* test (GraphPad Prism, version 6.03, GraphPad Software, La Jolla California USA, <http://www.graphpad.com>) to compare differences between radioconjugates injected in the same mice and an unpaired *t* test (GraphPad Prism, version 6.03) to compare differences between radioconjugates injected in separate mice. For multiple comparisons, 1-way analysis of variance (GraphPad Prism, version 6.03) was used. *P* values are indicated and considered significant when *P* < .5.

Results

Properties of Radiolabeled ch806 Antibodies

Radiochemical properties of radiolabeled ch806 antibodies are shown in Table 1. Radiolabeling efficiencies of radioiodinated

ch806 antibodies ranged from 23% to 70%, radiochemical purities ranged from 98.0% to 99.9%, and specific activities ranged from 22.2% to 48.1 MBq/mg. The binding properties of radioconjugates were initially determined using the Lindmo assay to ascertain conditions for maximal binding in the presence of antigen excess. We observed that maximal binding occurred at a cell concentration of 5 million cells/mL of media (see Figure 2). Subsequently, a single point assay using 10 million cells was deemed suitable to represent conditions for antigen excess (using 20 ng of radioconjugates) for comparing the immunoreactivities of the larger number of radioconjugates, ranging from 64.0% to 79.9% cell binding. Adding metabisulfite to the radiolabeled peptide mixture before conjugation to native antibody resulted in <0.1% radiolabeling indicating that it had stopped the iodination reaction. Little direct iodination took place. ^{111}In -CHX-A''-DTPA-ch806 was prepared with 80.4% radiolabeling efficiency, a specific activity of 44.4 MBq/mg, 99.6% radiochemical purity, and 74.6% cell binding in the presence of antigen excess. Results are summarized in Table 1.

Lindmo/Scatchard Analysis and Serum Stability of ^{124}I -PEG₄-tptddYddtpt-ch806

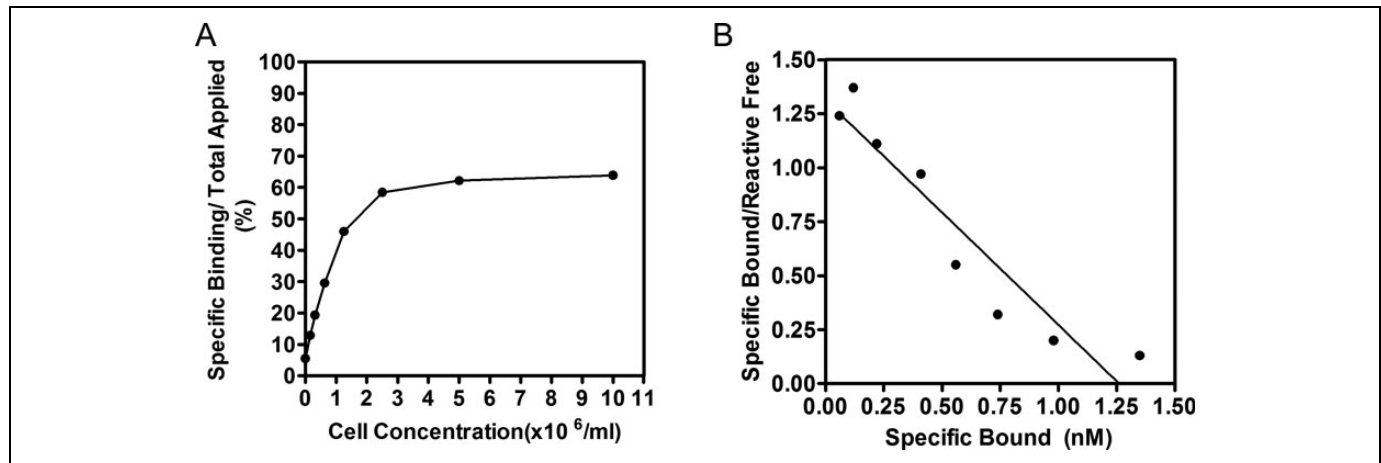
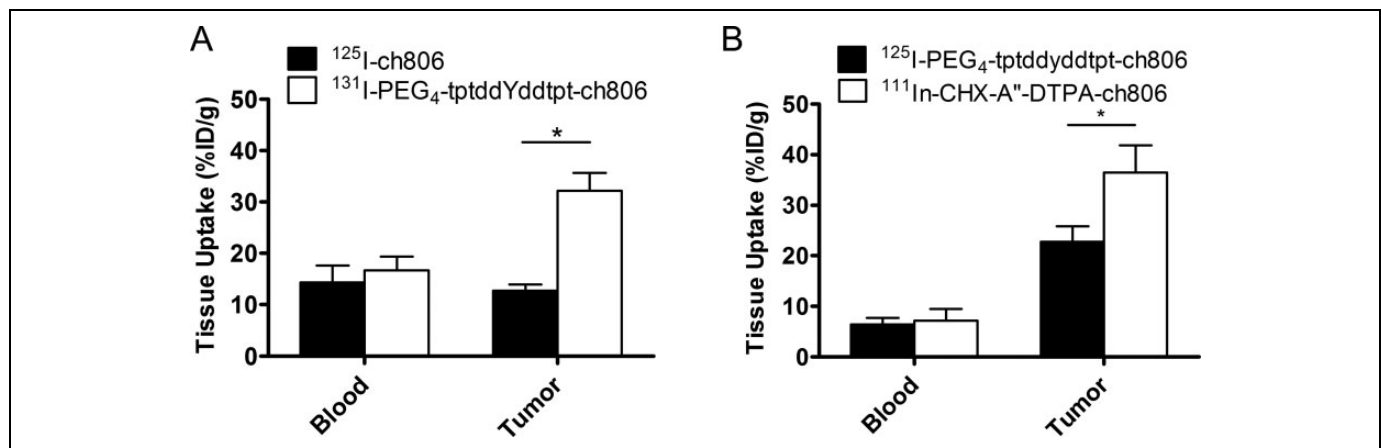
Radiolabeling efficiency of ^{124}I -PEG₄-tptddYddtpt-ch806 was 23.0%, radiochemical purity was 98.0%, specific activity was 25.9 MBq/mg, and immunoreactivity was 64% cell binding in the presence of antigen excess (Figure 2). Scatchard analysis determined that the apparent association constant of ^{124}I -tptddYddtpt-ch806 was $1.04 \times 10^9 \text{ M}^{-1}$, and the number of antibodies bound per cell was approximately 760 000. The stability of the radioconjugate was determined by a single-point immunoreactivity assay after incubation in human serum at 37 C. The immunoreactivity decreased from 64% on day 0, to 44.3% and 39.3% on days 3 and 7, respectively. An ITLC-SG analysis showed a modest decrease in radiochemical purity from 99.6% on day 0 to 93.0% and 87.9% on days 3 and 7, respectively.

Biodistribution

To screen for suitable residualizing peptides, the tumor uptake of various ch806 radioconjugates was compared using biodistribution studies at 72 hours postinjection only, corresponding to maximal tumor uptake previously observed with ^{111}In -CHX-A''-DTPA-ch806.¹⁰ Figure 3 summarizes the blood and tumor values (% ID/g) of these biodistribution studies. Uptake and retention of radioconjugates in tumors are ranked in following order: mixed D/L-11-mer (^{131}I -PEG₄-tptddYddtpt-ch806) comparable to ^{111}In (^{111}In -CHX-A''-DTPA-ch806) > all-D-11-mer (^{125}I -PEG₄-tptddyddtpt-ch806, > direct iodination (^{125}I -ch806). Because of this ranking, the D/L-11-mer was further employed in a full biodistribution study with ^{124}I . The ^{124}I -radioimmunoconjugate can be used for high-resolution imaging and determining dosimetry for a subsequent therapy with the ^{131}I -conjugate.

Table 1. Radiochemical Properties of Various ch806 Radioconjugates.

Radioconjugate	Radiolabeling Efficiency (%)	Specific Activity, MBq/mg	Radiochemical purity (%)	Immunoreactivity (% Binding)
^{125}I -ch806	70.0	44.4	99.9	77.2
^{131}I -PEG ₄ -tptddYddtpt-ch806	35.1	22.2	98.5	74.4
^{125}I -PEG ₄ -tptddyddtpt-ch806	28.5	48.1	98.5	79.9
^{111}In -CHX-A''-DTPA-ch806	80.4	44.4	99.6	74.6
^{124}I -tptddYddtpt-ch806	23.0	25.9	98.0	64.0

**Figure 2.** Binding assay for the determination of immunoreactive fraction of an ^{124}I -tptddYddtptch806 antibody binding to U87MG.de2-7 cells. Panel A shows a conventional plot of specific binding over applied radioactivity as a function of increasing cell concentration (Lindmo assay). Panel B shows a Scatchard plot of binding of radioconjugates to the same cells. The abscissa shows the concentration of specifically bound antibody and the ordinate, the ratio of the concentrations of specifically bound over reactive-free antibody.**Figure 3.** Blood and tumor uptake (% ID/g) of various ch806 radioconjugates in U87MG.de2-7 tumor-bearing mice at 72 hours after injection. Results of biodistribution of ^{125}I -ch806 and ^{131}I -PEG₄-tptddYddtpt-ch806 (A) and ^{125}I -PEG₄-tptddyddtpt-ch806 and ^{111}In -CHX-A''-DTPA-ch806 (B). Bars, SD; n = 5; *P < .005. SD indicates standard deviation.

The biodistribution properties of ^{124}I -PEG₄-tptddYddtpt-ch806 in xenografted mice over 7 days are shown in Table 2. The mean uptake of ^{124}I -PEG₄-tptddYddtpt-ch806 by U87MG.de2-7 tumors reached a maximum of $36.03\% \pm 5.08\%$ ID/g at 72 hours after injection, when tumor sizes were 528.20 ± 75.58 mg. The tumor uptake decreased to $7.44 \pm$

1.84% ID/g by day 7 after injection. The tumor-to-blood ratios increased from 0.32 ± 0.02 (at 2 hours after injection) to 8.18 ± 1.82 at 72 hours after injection and continued to increase to a high of 35.84 ± 19.47 at 168 hours postinjection. Uptake in normal tissues (eg, kidney and liver) was low, with a time-dependent decrease paralleling that in the blood (Table 2).

Table 2. Biodistribution of ^{124}I -PEG₄-tptddYddtpt-ch806 in BALB/c Nude Mice-Bearing U87MG.de2-7 Xenografts.^a

Tissue	Time, hours					
	2	24	48	72	120	168
Blood	28.84 ± 1.37	11.49 ± 1.37	4.99 ± 1.67	4.47 ± 0.38	0.78 ± 0.16	0.22 ± 0.08
Brain	0.88 ± 0.19	0.39 ± 0.09	0.20 ± 0.05	0.23 ± 0.05	0.10 ± 0.02	0.09 ± 0.02
Heart	7.85 ± 1.10	3.02 ± 0.50	1.53 ± 0.42	1.72 ± 0.41	0.56 ± 0.08	0.52 ± 0.10
Lung	9.79 ± 1.04	4.17 ± 0.45	2.29 ± 0.55	2.51 ± 0.21	0.96 ± 0.45	0.53 ± 0.11
Stomach	17.39 ± 2.95	1.52 ± 0.36	1.31 ± 0.38	1.11 ± 0.20	0.48 ± 0.14	0.29 ± .080
Spleen	5.23 ± 0.93	3.18 ± 0.42	3.46 ± 0.47	3.68 ± 1.04	1.94 ± 0.58	1.50 ± 0.36
Liver	7.53 ± 0.63	4.79 ± 0.58	4.28 ± 1.08	4.03 ± 0.29	2.12 ± 0.37	1.77 ± 0.32
Kidney	7.48 ± 0.34	4.18 ± 0.36	4.32 ± 0.37	4.49 ± 0.48	3.91 ± 0.59	4.79 ± 1.21
Small intestine	3.19 ± 0.28	1.03 ± 0.09	0.68 ± 0.18	0.66 ± 0.13	0.22 ± 0.06	0.15 ± 0.03
Colon	2.26 ± 0.25	1.02 ± 0.14	0.65 ± 0.16	0.76 ± 0.11	0.31 ± 0.07	0.29 ± 0.16
Muscle	1.48 ± 0.25	1.07 ± 0.13	0.77 ± 0.15	0.66 ± 0.05	0.31 ± 0.07	0.23 ± 0.05
Bone	3.99 ± 0.85	2.01 ± 0.23	1.41 ± 0.27	2.69 ± 1.14	0.91 ± 0.19	1.33 ± 1.23
Skin	4.22 ± 0.47	2.96 ± 0.28	2.19 ± 0.43	1.78 ± 0.26	1.09 ± 0.26	0.85 ± 0.20
Tail	4.53 ± 0.95	2.54 ± 0.35	1.19 ± 0.23	1.06 ± 0.29	0.59 ± 0.07	0.37 ± 0.13
Tumor	9.44 ± 0.78	34.41 ± 7.24	33.55 ± 5.48	36.03 ± 5.08	13.12 ± 2.86	7.44 ± 1.84

^aData presented are % ID/g tissue values (mean ± standard deviation [SD]; n = 5).

There was some transient activity in the stomach, which cleared rapidly. The serum half-life of the initial phase of disposition ($t_{1/2\alpha}$) was 1.95 ± 0.63 hours, the terminal half-life ($t_{1/2\beta}$) was 25.96 ± 5.29 hours, the area under the curve (AUC) was 46.23 ± 4.56 h· $\mu\text{g}/\text{mL}$, and the total serum clearance was 0.11 ± 0.01 mL/h. The AUC for tumor was 186.13 ± 18.31 h \times $\mu\text{g}/\text{mL}$, providing a tumor-to-blood ratio for AUC of 4.03. On day 7, the biodistribution properties of the imaging dose (74 $\mu\text{g}/1.92$ MBq) in 5 mice were similar to the lower dose (5 $\mu\text{g}/0.13$ MBq; Table 2). The % ID/g values were as follows: blood (0.54 ± 0.21), brain (0.05 ± 0.03), heart (0.46 ± 0.09), lung (0.79 ± 0.20), stomach (0.35 ± 0.07), spleen (2.25 ± 0.42), liver (2.71 ± 0.31), kidney (6.97 ± 1.58), small intestine (0.19 ± 0.03), colon (0.28 ± 0.14), muscle (0.20 ± 0.04), bone (0.90 ± 1.07), skin (0.87 ± 0.19), and tumor (12.79 ± 3.2). The exceptions were values for blood and tumor. Blood: 0.54 ± 0.21 vs 0.22 ± 0.09 vs 0.54 ± 0.21 % ID/g ($P = .0141$) and tumor: 12.79 ± 0.88 vs 7.44 ± 2.05 % ID/g ($P = .0007$). The significantly higher values of the imaging doses in blood and tumor were likely to be related to the higher protein dose used.

Positron Emission Tomography/Magnetic Resonance Imaging

Tumor uptake of ^{124}I -PEG₄-tptddYddtpt-ch806 was evident at 72 hours as shown by the fused PET and MR surface-rendered image, together with coronal and transaxial images (Figure 4). Clearance of blood pool activity with time, and some thyroid and abdominal uptake, is consistent with the pharmacokinetics and catabolic pathways of radioiodinated intact antibodies. The average thyroid uptake values of 2 of 5 mice one of which is shown in Figure 4 were day 0 (0.09 g/mL), day 2 (0.14 g/mL), and day 7 (0.05 g/mL). The corresponding tumor values were day 0 (0.27 g/mL), day 2 (1.27 g/mL), and day 7 (0.63 g/mL). No other normal tissue uptake was observed at the later time

points, consistent with the biodistribution study on tissues obtained by radioactive counting of blood and tissues. Coronal and transaxial plane views of PET/MRI image data sets confirmed high uptake of ^{124}I -PEG₄-tptddYddtpt-ch806 by the tumor (Figure 4).

Discussion

In recent years, with the availability of ^{89}Zr and suitable bifunctional metal ion chelates, immuno-PET has more and more been used in early-phase cancer clinical trials.^{4,5,31} The PET isotope ^{124}I , which has a comparable decay half-life and is suitable for long half-life antibodies, has also been used but has been restricted to antibodies that are not extensively internalized and catabolized which avoids dehalogenation from intracellular enzymes.³² In an attempt to trap radioiodinated catabolites in lysosomes, various strategies have been developed.¹⁶⁻²⁸ A DTPA-appended D-amino acid-containing peptide IMP-R4 was used before to label ch806 with ^{124}I and demonstrated targeting and biodistribution properties comparable to ^{111}In -CHX-A''-DTPA-ch806 in U87MG.de2-7 xenografts.¹¹

In this study, a D-amino acid-rich peptide for residualizing radioiodine labeling, PEG₄-DThr-DPro-DThr-DAsp-DAsp-Tyr-DAsp-DAsp-DThr-DPro-DThr (PEG₄-tptddYddtpt), was designed based on the known contribution of proline motifs and D-amino acids in resisting proteolytic degradation of peptides^{29,33} and the observation that the use of a flanking D-amino acid motif DThr-DPro-DThr protects a central L-amino acid peptide sequence from proteolytic degradation.²⁹ This peptide has the advantage that it is easily accessible, and relatively simple conjugation chemistry is needed to link the peptide to the antibody. Some residualizing properties were observed when a central all-D-amino acid pentapeptide (PEG₄-tptddyddtpt) was employed, but tumor uptake of ^{124}I -PEG₄-tptddyddtpt-ch806 was substantially less than that for the corresponding

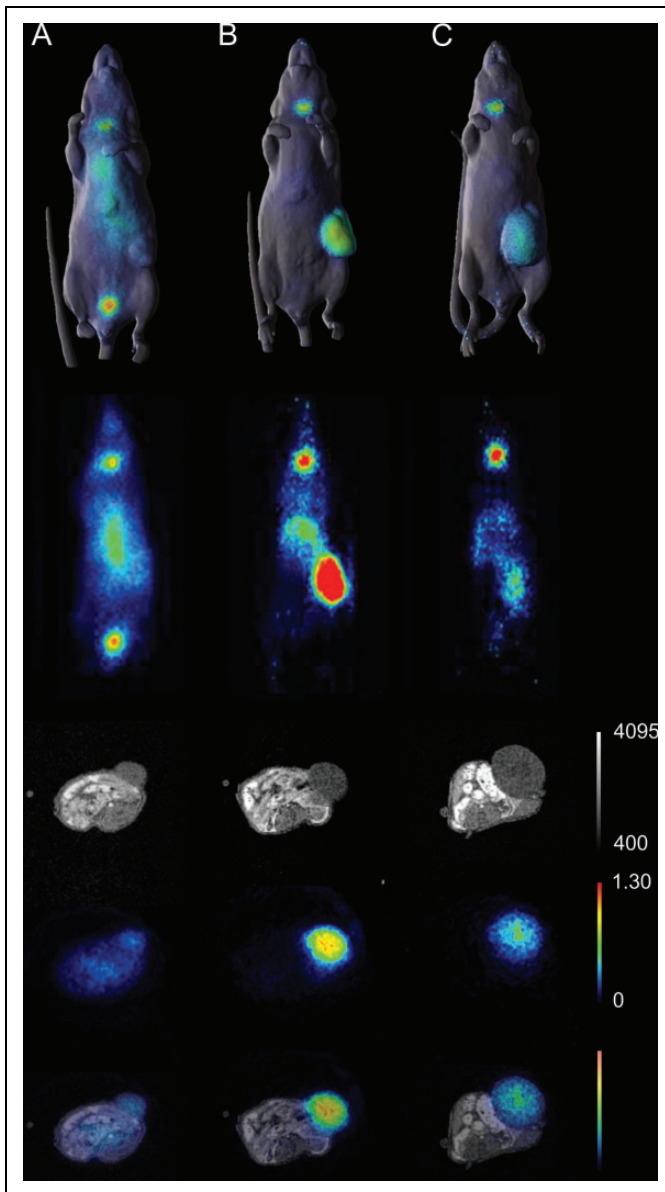


Figure 4. Example of fused PET (maximum intensity projection)/MRI (T1-weighted surface rendered) images of U87MG.de2-7 tumor-bearing mice taken at 2 (A), 72 (B) and 168 hours (C) after injection of ^{124}I -PEG₄-tptddYddtpt-ch806 showing uptake of radioconjugates in U87MG.de2-7 tumor in the left flank at 72 and 168 hours after injection. Corresponding coronal and transaxial images are also shown (top-bottom). PET indicates positron emission tomography; MRI, magnetic resonance imaging.

^{111}In -conjugate. When L-tyrosine substitution was employed in the central all-D-pentapeptide, the observed tumor uptake of ^{124}I -PEG₄-tptddYddtpt-ch806 was similar to the ^{111}In -conjugate.

The present study showed that ^{124}I -PEG₄-tptddYddtpt-ch806 could be radiolabeled efficiently and maintained radiochemical purity for up to 7 days. Although the immunoreactivity of ^{124}I -PEG₄-tptddYddtpt-ch806 declined with time, the results are consistent with other immunoconjugates successfully applied in the clinic.^{34,35} ^{124}I -PEG₄-tptddYddtpt-

ch806 showed biodistribution properties and tumor retention in U87MG.de2-7 xenografts similar to that of ^{111}In -CHX-A''-DTPA-ch806¹⁰ and ^{124}I -IMP-R4-ch806.¹¹ In terms of clinical applications, this peptide should be useful for immuno-PET. Doses of up to 185 to 370 MBq of directly radiolabeled ^{124}I -antibodies such as cG250 have been successfully used for immuno-PET in the clinic,^{36,37} with preclinical tumor uptake of radioiodinated cG250 similar to as observed with ^{124}I -PEG₄-tptddYddtpt-ch806. These doses can be obtained with the current labeling efficiency observed (23.0%-35.1%). This peptide is a first-generation reagent, and modifications can be made to improve radiolabeling yields. In one instance, the more recent click chemistry pair of transcyclooctene and tetrazine linkage is reported to be more efficient compared to the present DBCO and azido linkage. We have also introduced the use of soluble tyrosine peptides (ddYdd or DDYDD) to quench the iodination reaction before adding derivatized antibody. These measures will likely improve the overall radiolabeling efficiency of radioiodination.

^{124}I -PEG₄-tptddYddtpt-ch806 showed a 3-fold increase in tumor uptake compared to directly radioiodinated ^{125}I -ch806, and tumor-to-blood ratios increased from 0.32:1 at 2 hours after injection to 35.84:1 at 168 hours after injection. These values are similar to values found with other improved D-amino acid-containing residualizing labels for radioiodination of monoclonal antibodies.^{11,25-28} In addition, ^{124}I -PEG₄-tptddYddtpt-ch806 showed low renal uptake compared to other residualizing labels (eg, renal uptake at 24 hours after injection: D-KRYRR, $10.51 \pm 1.69\%$ ID/g²⁵; IB-Mal-D-GEEEK, $9.75 \pm 1.16\%$ ID/g²⁶ vs PEG₄-tptddYddtpt, $4.18 \pm 0.36\%$ ID/g; $P < .05$).

The potential effect of peptide modifications of ch806 antibody on changes in physical, chemical, and subsequent biodistribution properties should be minimal. In our previous studies,^{10,11} we have shown that using low conjugation ratio between ligand and antibody did not alter properties in a measurable way. Derivatizing ch806 with the bifunctional metal ion chelate CHX-A''-DTPA (approx molecular weight 1200), containing 5 negative charges, did not alter the biodistribution properties of the ^{111}In -CHX-A''-DTPA ch806 compared to the reference standard ^{125}I -ch806 in terms of pharmacokinetics and tissue distribution (except for tumor uptake).¹⁰ Subsequently, we performed a similar study using a residualizing peptide IMP-R4, containing 10 negative charges, to modify the same antibody ch806. Biodistribution studies again showed similar uptake of ^{124}I -IMP-ch806 in tumors and normal tissues,¹¹ comparable to the well-documented ^{111}In -CHX-A''-DTPA ch806.¹⁰

Our present study used DBCO-PEG4-NHS (molecular weight 649.68) to derivatize the antibody. The PEG4 would have reduced the lipophilicity of DBCO. As the conjugation ratio is again kept low as before, no more than 2 or 3 molecules are expected to be attached to the antibody (molecular weight 150 000). The radioiodinated residualizing peptide-containing 4 D-aspartic acid residues (4 negative charges, molecular weight 1500), used for attaching to DBCO-ch806, would have

further reduced the lipophilicity of DBCO somewhat, as would have the PEG molecules. As the molecular weight of the modification agents are small and few in numbers, they are unlikely to significantly alter the biodistribution properties of the much larger antibody molecule.

The exact mechanism by which ^{124}I -PEG₄-tptddYddtpt-ch806 accumulates in tumor cells is as yet unknown. D-Amino acid-metabolizing enzymes have been reported,^{38,39} suggesting that mammalian tissues have the ability to metabolize D-aspartic acid-containing proteins. D-Aspartic acid-containing proteins can be metabolized by 1 or more enzymes (eg, D-aspartyl endopeptidase purified from rabbit liver, cleaves D-aspartate-containing proteins at the carbonyl side of this residue).³⁸ On the other hand, lysosomal enzymes such as cathepsins are known to catalyze the breakdown of L-amino acid enantiomeric proteins within lysosomes.⁴⁰ Results of the current study suggest that the tptddYddtpt peptide was able to resist proteolysis by these 2 groups of D- and L-metabolizing enzymes. To gain insight into the residualizing properties of the peptide, the effect of modifications such as D-threonine residue substitution and shortening of the peptide are currently being examined.

Conclusions

The present study shows that a mixed D/L-enantiomeric peptide, DThr-DPro-DThr-DAsp-DAsp-Tyr-DAsp-DAsp-DThr-DPro-DThr, is suitable for radiolabeling of antibodies with radiohalogens such as ^{124}I for high-resolution immuno-PET imaging of tumors and for evaluating biodistribution and tumor-targeting properties of antibodies in early-phase clinical trials.

Acknowledgments

The authors wish to thank Ms Rose Bogdal and Mrs Malarmarthy Ramachandran for technical assistance in binding assays and biodistribution studies.

Declaration of Conflicting Interests

The author(s) declared no potential conflicts of interest with respect to the research, authorship, and/or publication of this article.

Funding

The author(s) disclosed receipt of the following financial support for the research, authorship, and/or publication of this article: This study was supported in part by NHMRC Project grant 1003085 and NHMRC Program grant 487922. Operational Infrastructure Support Program funding was provided by the Victorian Government and funds to purchase the imaging equipment was provided by the Australian Cancer Research Foundation.

Supplemental Material

The online (appendices/data supplements/etc) are available at <http://mix.sagepub.com/supplemental>.

References

1. Scott AM, Wolchok JD, Old LJ. Antibody therapy of cancer. *Nat Rev Cancer*. 2012;12(4):278-287.
2. Sliwkowski MX, Mellman I. Antibody therapeutics in cancer. *Science*. 2013;341(6151):1192-1198.
3. Nagengast WB, de Vries EG, Hospers GA, et al. In vivo VEGF imaging with radiolabeled bevacizumab in a human ovarian tumor xenograft. *J Nucl Med*. 2007;48(8):1313-1319.
4. Verel I, Visser GW, van Dongen GA. The promise of immuno-PET in radioimmunotherapy. *J Nucl Med*. 2005;46(suppl 1):164s-171s.
5. Knowles SM, Wu AM. Advances in immuno-positron emission tomography: antibodies for molecular imaging in oncology. *J Clin Oncol*. 2012;30(31):3884-3892.
6. Pillay V, Gan HK, Scott AM. Antibodies in oncology. *N Biotechnol*. 2011;28(5):518-529.
7. Burgess AW. EGFR family: structure physiology signalling and therapeutic targets. *Growth Factors*. 2008;26(5):263-274.
8. Johns TG, Stockert E, Ritter G, et al. Novel monoclonal antibody specific for the de2-7 epidermal growth factor receptor (EGFR) that also recognizes the EGFR expressed in cells containing amplification of the EGFR gene. *Int J Cancer*. 2002;98(3):398-408.
9. Gan HK, Burgess AW, Clayton AH, Scott AM. Targeting of a conformationally exposed, tumor-specific epitope of EGFR as a strategy for cancer therapy. *Cancer Res*. 2012;72(12):2924-2930.
10. Panousis C, Rayzman VM, Johns TG, et al. Engineering and characterisation of chimeric monoclonal antibody 806 (ch806) for targeted immunotherapy of tumours expressing de2-7 EGFR or amplified EGFR. *Br J Cancer*. 2005;92(6):1069-1077.
11. Lee FT, O'Keefe GJ, Gan HK, et al. Immuno-PET quantitation of de2-7 epidermal growth factor receptor expression in glioma using ^{124}I -IMP-R4-labeled antibody ch806. *J Nucl Med*. 2010;51(6):967-972.
12. Gan HK, Burge ME, Solomon BJ, et al. A phase I and biodistribution study of ABT-806i, an ^{111}In -labeled conjugate of the tumor-specific anti-EGFR antibody ABT-806. *J Clin Oncol*. 2013;31 suppl:abstract 2520.
13. Scott AM, Tebbutt N, Lee FT, et al. A phase I biodistribution and pharmacokinetic trial of humanized monoclonal antibody Hu3s193 in patients with advanced epithelial cancers that express the Lewis-Y antigen. *Clin Cancer Res*. 2007;13(11):3286-3292.
14. Shih LB, Thorpe SR, Griffiths GL, et al. The processing and fate of antibodies and their radiolabels bound to the surface of tumor cells in vitro: a comparison of nine radiolabels. *J Nucl Med*. 1994;35(5):899-908.
15. Mattes MJ, Griffiths GL, Diril H, Goldenberg DM, Ong GL, Shih LB. Processing of antibody-radioisotope conjugates after binding to the surface of tumor cells. *Cancer*. 1994;73(suppl 3):787-793.
16. Stein R, Goldenberg DM, Thorpe SR, Basu A, Mattes MJ. Effects of radiolabeling monoclonal antibodies with a residualising iodine radiolabel on the accretion of radioisotope in tumors. *Cancer Res*. 1995;55(14):3132-3139.
17. Thorpe SR, Baynes JW, Chronos ZC. The design and application of residualising labels for studies of protein catabolism. *FASEB J*. 1993;7(5):399-405.
18. Ali SA, Warren SD, Richter KY, et al. Improving the tumor retention of radioiodinated antibody: aryl carbohydrate adducts. *Cancer Res*. 1990;50(suppl 3):783s-788s.

19. Ali SA, Eary JF, Warren SD, Badger CC, Krohn KA. Synthesis and radioiodination of tyramine cellobiose for labeling monoclonal antibodies. *Int J Rad Appl Instrum B*. 1988;15(5):557-561.
20. Maxwell JL, Baynes JW, Thorpe SR. Inulin-125I-tyramine, an improved residualising label for studies on sites of catabolism of circulating proteins. *J Biol Chem*. 1988;263(28):14122-14127.
21. Pittman RC, Carew TE, Glass CK, Green SR, Taylor CA Jr, Attie AD. A radioiodinated, intracellularly trapped ligand for determining the sites of plasma protein degradation in vivo. *Biochem J*. 1983;212(3):791-800.
22. Reist CJ, Garg PK, Alston KL, Bigner DD, Zalutsky MR. Radioiodination of internalizing monoclonal antibodies using N-succinimidyl 5-iodo-3-pyridinecarboxylate. *Cancer Res*. 1996;56(21):4970-4977.
23. Vaidyanathan G, Affleck DJ, Bigner DD, Zalutsky MR. Improved xenograft targeting of tumor-specific anti-epidermal growth factor receptor variant III antibody labeled using N-succinimidyl 4-guanidinomethyl-3-iodobenzoate. *Nucl Med Biol*. 2002;29(1):1-11.
24. Shankar S, Vaidyanathan G, Affleck DJ, Peixoto K, Bigner DD, Zalutsky MR. Evaluation of an internalizing monoclonal antibody labeled using N-succinimidyl 3-[¹³¹I]iodo-4-phosphononmethylbenzoate ([¹³¹I]SIPMB), a negatively charged substituent bearing acylation agent. *Nucl Med Biol*. 2004;31(7):909-919.
25. Foulon CF, Welsh PC, Bigner DD, Zalutsky MR. Positively charged templates for labeling internalizing antibodies: comparison of N-succinimidyl 5-iodo-3-pyridinecarboxylate and the D-amino acid peptide KRYRR. *Nucl Med Biol*. 2001;28(7):769-777.
26. Vaidyanathan G, Alston KL, Bigner DD, Zalutsky MR. Nepsilon-(3-[¹²⁵I]iodobenzoyl)-Lys5-Nalpha-maleimido-Gly1-GEEEEK ([¹²⁵I]IB-Mal-D-GEEEEK): a radioiodinated prosthetic group containing negatively charged D-glutamates for labeling internalizing monoclonal antibodies. *Bioconjug Chem*. 2006;17(4):1085-1092.
27. Govindan SV, Mattes MJ, Stein R, et al. Labeling of monoclonal antibodies with diethylenetriaminepentaacetic acid-appended radioiodinated peptides containing D-amino acids. *Bioconjug Chem*. 1999;10(2):231-240.
28. Stein R, Govindan SV, Mattes MJ, et al. Improved iodine radiolabels for monoclonal antibody therapy. *Cancer Res*. 2003;63(1):111-118.
29. Tugyi R, Uray K, Ivan D, Fellingner E, Perkins A, Hudecz F. Partial D-amino acid substitution: improved enzymatic stability and preserved Ab recognition of a MUC2 epitope peptide. *Proc Natl Acad Sci U S A*. 2005;102(2):413-418.
30. Lee FT, Rigopoulos A, Hall C, et al. Specific localization, gamma camera imaging, and intracellular trafficking of radiolabeled chimeric anti-G(D3) ganglioside monoclonal antibody KM871 in SK-MEL-28 melanoma xenografts. *Cancer Res*. 2001;61(11):4474-4482.
31. Wright BD, Lapi SE. Designing the magic bullet? The advancement of immuno-PET into clinical use. *J Nucl Med*. 2013;54(8):1171-1174.
32. Verel I, Visser GW, Boerman OC, et al. Long-lived positron emitters zirconium-89 and iodine-124 for scouting of therapeutic radioimmunoconjugates with PET. *Cancer Biother Radiopharm*. 2003;18(4):655-661.
33. Walker JR, Altman RK, Warren JW, Altman E. Using protein-based motifs to stabilize peptides. *J Pept Res*. 2003;62(5):214-226.
34. Scott AM, Lee FT, Jones R, et al. A phase I trial of humanized monoclonal antibody A33 in patients with colorectal carcinoma: biodistribution, pharmacokinetics, and quantitative tumor uptake. *Clin Cancer Res*. 2005;11(13):4810-4817.
35. Scott AM, Lee FT, Tebbutt N, et al. A phase I clinical trial with monoclonal antibody ch806 targeting transitional state and mutant epidermal growth factor receptors. *Proc Natl Acad Sci U S A*. 2007;104(10):4071-4076.
36. Schwartz J, Humm JL, Divgi CR, Larson SM, O'Donoghue JA. Bone marrow dosimetry using ¹²⁴I-PET. *J Nucl Med*. 2012;53(4):615-621.
37. Divgi CR, Pandit-Taskar N, Jungbluth AA, et al. Preoperative characterisation of clear-cell renal carcinoma using iodine-124-labelled antibody chimeric G250 (124I-cG250) and PET in patients with renal masses: a phase I trial. *Lancet Oncol*. 2007;8(4):304-310.
38. Yamada RH, Kera Y, Takahashi S. Occurrence and functions of free D-aspartate and its metabolizing enzymes. *Chem Rec*. 2006;6(5):259-266.
39. Homma H. Biochemistry of D-aspartate in mammalian cells. *Amino Acids*. 2007;32(1):3-11.
40. Schulze H, Kolter T, Sandhoff K. Principles of lysosomal membrane degradation: cellular topology and biochemistry of lysosomal lipid degradation. *Biochim Biophys Acta*. 2009;1793(4):674-683.